Global reaction heat of acetic acid oxidation in supercritical water

Cyril Aymonier, Aurélia Gratias, Jacques Mercadier, François Cansell

Global reaction heat of acetic acid oxidation in supercritical water

C. Aymonier [a], A. Gratias [a], J. Mercadier [b], F. Cansell [a,*]

[a] *Institut de Chimie de la Matière Condensée de Bordeaux (I.C.M.C.B), CNRS-UPR 9048, Université Bordeaux I, 87 Avenue du Dr Albert Schweitzer, 33608 Pessac Cedex, France*

[b] *Ecole Nationale Supérieure en Génie des Technologies Industrielles (E.N.S.G.T.I), E.A. 1932, Université de Pau, Rue Jules Ferry, 64000 Pau, France*

Abstract

The scaling-up of hydrothermal oxidation process is performed by the use of simulation tools, which require an important experimental support. In this way, we have proposed a new experimental approach to determine the global reaction heats of hydrothermal oxidation reactions. A quasi-adiabatic tubular reactor was developed in order to follow the temperature profiles along the reactor during the oxidation reaction. From the experimental temperature profiles, a model of the reactor thermal behavior was proposed and gives access to the global reaction heats. The experimental setup and model have been validated for acetic acid oxidation in supercritical water with hydrogen peroxide as oxidant. The global reaction heat of acetic acid hydrothermal oxidation ($P = 25$ MPa, $400 \leq T \leq 570$ °C) has been found equal to -925 kJ mol^{-1}.

Keywords: Hydrothermal oxidation; Temperature profile; Reactor simulation; Acetic acid; Global reaction heat

1. Introduction

Industrial societies generate increasing quantities of organic wastewaters and sludges, which require disposal or destruction. Disposal has usually been achieved in landfills, but this practice will rapidly become quite expensive and very restricting. An important research work has been undertaken to develop new technologies in order to achieve four major aims: valorization, decomposition in environmentally acceptable end products, final volume reduction of wastes, and reduction of energy consumption. Among the alternative practices, hydrothermal oxidation, and more precisely Supercritical Water Oxidation (SCWO), is being investigated as a method for destroying liquid wastes and sludges [1–4]. End products resulting from hydrothermal conversion are essentially water and mineral acids (HCl, H_2SO_4, H_3PO_4,...) in liquid phase, carbon dioxide and molecular nitrogen in gas phase [5]. Numerous studies describe the reactive pathway of the hydrothermal oxidation of model molecules and industrial wastes: acetic acid [6],

* Corresponding author. Tel.: +33-55-684-2673; fax: +33-55-684-2761.

E-mail address: cansell@icmcb.u-bordeaux.fr (F. Cansell).

methanol [7], phenol [8], pyridine [9], pulp mill sludges [10], etc.

Due to the supercritical water properties [11–13], both organic matter and oxidant (air, oxygen or hydrogen peroxide) are completely miscible with water [14,15], so that interfacial transport phenomena are suppressed. In this way, high destruction rates of wastes can be obtained in relatively short reaction times with a Chemical Oxygen Demand (COD) reduction greater than 99.9% [1]. However, the solubility of inorganic salts drops to the parts per million (ppm) range [16]. So, inorganic salts precipitate and can deposit on reactor and heat exchanger surfaces. Moreover, corrosion of SCWO reactor materials by highly corrosive aqueous environment is also a major factor, which must be taken into account, for the development of SCWO processes [17]. In these conditions, many new concepts of reactors have been developed to overcome salt precipitation and corrosion [18–23].

In parallel, for scaling-up hydrothermal oxidation process [24–26], numerous research teams have worked on the development of simulation tools. In fact, two parts of the process require a precise model: the reactor and the heat exchanger. However, the knowledge of parameters, which characterize the process operation, is necessary for the development of simulation tools. These data are essentially hydrothermal oxidation chemical pathway, reaction kinetic and thermal parameters (reactive mixture thermodynamic properties (fluid specific calorific capacity) and heat transfer coefficients). Even if chemical pathways and kinetic parameters of hydrothermal oxidation reactions are well documented [6,27,28], only few works concern thermal parameters. Chen et al. [29] proposed an average reaction heat of -435 kJ mol^{-1} for most organic compounds and -870 kJ mol^{-1} for acetic acid. Similar result of reaction heat (-847 kJ mol^{-1}) was found with Prophy Plus, a simulation computer software package, for the acetic acid hydrothermal oxidation with oxygen [30]. However, the equation of state used was established for pressures lower than 15 MPa.

So, we propose a new experimental approach to determine global reaction heats of hydrothermal oxidation reactions. The global reaction heat evaluation is based on: (i) a quasi-adiabatic tubular reactor developed at ICMCB, which allows to measure the temperature distribution along the reactor, (ii) a modeling of this reactor to exploit the experimental temperature profiles and so to calculate the global reaction heat.

In this paper, the global reaction heat of acetic acid hydrothermal oxidation has been determined.

After a description of the quasi-adiabatic tubular reactor, the obtained temperature profiles for acetic acid hydrothermal oxidation are discussed. A model of the reactor is proposed to calculate acetic acid global reaction heat.

2. Experimental section

2.1. Quasi-adiabatic tubular reactor

The quasi-adiabatic tubular reactor was developed to determine the heat quantity produced by hydrothermal oxidation reactions of model molecules and industrial wastes. The quasi-adiabatic tubular reactor (Fig. 1) was made of Inconel 718 tube of 2.4 mm inside diameter and 8.4 m length (volume of 38 ml). It was equipped with 28 thermocouples (type K) distributed along the reactor. Generally, the temperature increase takes place in the first part of reactor. In this way, more thermocouples were distributed in the first part of

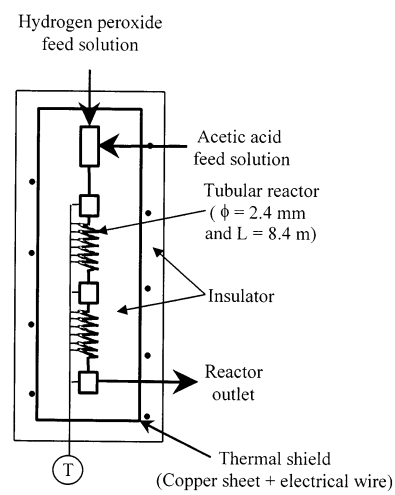

Fig. 1. Quasi-adiabatic tubular reactor.

Table 1
Hydrothermal oxidation of acetic acid at 25 MPa

Run	$T_{injection}$ (°C)	D (kg h^{-1})	t_r (s)	A.Ac.$_{initial}$ (% w/wt)	X (%)
A1	395	0.5	34.2	3.35	30.5
A2	392	0.5	26.4	3.92	98.4
A3	403	0.5	24.6	4.90	96.9

$T_{injection}$ = the temperature at the quasi-adiabatic tubular reactor inlet (just after the mixing of acetic acid and hydrogen peroxide feed solutions), D = the mass flow rate at the reactor inlet, t_r = the residence time in the reactor, A.Ac$_{initial}$ = the weight concentration of acetic acid at the reactor inlet, and X = the acetic acid conversion rate.

the reactor than in the second part. The tube was isolated with ceramic fiber and surrounded with a thermal shield. The thermal shield constituted a copper sheet surrounded with electrical heating in order to reduce thermal loss. The quasi-adiabatic tubular reactor allowed to obtain a temperature profile along the tube which characterized the exothermic oxidation reaction. This continuous reactor was built to work up to 50 MPa and 600 °C.

The quasi-adiabatic tubular reactor was adapted to the ICMCB continuous pilot plant facility, described elsewhere [5], whose the capacity reaches 3 kg h^{-1}. The residence time in the reactor was calculated from the software Labview.

Acetic acid feed solution (CH_3COOH at 99–100% from J.T. Baker in de-ionized water) and hydrogen peroxide feed solution (H_2O_2 at 35% from Fluka in de-ionized water) were pumped with high pressure pumps (LEWA). Acetic acid feed solution was pre-heated and mixed to a hydrogen peroxide feed solution (not pre-heated) at the reactor inlet. When it left the reactor, the reactive mixture was quenched in a water-cooled heat exchanger and the pressure reduced to atmospheric pressure. Liquid and gas phases were separated in a gas/liquid separator.

2.2. Analytical material and method

Acetic acid concentration in both feed and effluent liquid phase was measured by High Performance Ionic Chromatography (HPIC) with a Dionex DX 120 apparatus (column system: ion Pac AS 12A 4 mm + ion Pac AG 12 4 mm). Elution was performed at a flow rate of 1 ml min^{-1} using the following mobile phase: 2.7 mmol l^{-1} Na_2CO_3/0.3 mmol l^{-1} $NaHCO_3$. The measure accuracy was evaluated at $\pm$ 3%.

A COD measure was also performed in feed and effluent liquid phase. The sample was heated two hours with a powerful oxidant (potassium dichromate). Oxidable organic matter reduced Cr^{6+} ions into Cr^{3+} ions. The quantity of produced Cr^{3+} ions was measured by colorimetry. The measure accuracy was equal to $\pm$ 5%.

The gas effluent composition was analyzed on line by Gas Chromatography (GC) with a Varian star 3600CX apparatus (column system: Porapaq Q + molecular sieve 13 ×). Helium was used as carrier gas (He flow = 30 ml min^{-1}). The apparatus was equipped with a thermal conductivity detector. The temperatures of injector, column and detector were respectively 150, 40 and 180 °C.

3. Results and discussion

Acetic acid oxidation with hydrogen peroxide as oxidizer was studied at 25 MPa. H_2O_2 quantity was brought in stoichiometry, as calculated from the following equation:

$$CH_3COOH + 4H_2O_2 \rightarrow 2CO_2 + 6H_2O \quad (1)$$

Oxidation runs were performed with a solution injection temperature at the tubular reactor inlet close to 400 °C. The concentration of acetic acid at the reactor inlet, just after the mixing of acetic acid and hydrogen peroxide feed solutions, ranged between 3.35 and 4.90% w/wt. The run conditions and acetic acid conversion rates are summarized in Table 1. The conversion rate is defined from the following equation:

$$X = \frac{F - F'}{F} \quad (2)$$

where X, the conversion rate, F and F', the initial and final acetic acid molar fluxes. We only present the acetic acid conversion rate because the results obtained with COD analysis were well correlated. In fact, byproduct formation in liquid phase during acetic acid hydrothermal oxidation was negligible and acetic acid was transformed into H_2O and CO_2 [6].

3.1. Experimental temperature profiles

The temperature profiles obtained with the quasi-adiabatic tubular reactor for the different runs are reported in Fig. 2.

The injection temperature at the reactor inlet, just after the mixing of acetic acid and hydrogen peroxide feed solutions, was maintained to 400 °C. The quasi-adiabatic tubular reactor is surrounded with a thermal shield (see Section 2.1). The temperature of the thermal shield was uniform for the run A1 and equal to 400 °C. A temperature gradient of 100 °C between the reactor inlet and the reactor outlet (400 °C at the reactor inlet and 500 °C at the reactor outlet) was imposed for the runs A2 and A3 to reduce the gradient between the reactive mixture temperature and the thermal shield temperature at the reactor outlet.

Two kinds of temperature profiles were obtained (Fig. 2). For runs A2 and A3, the evolution

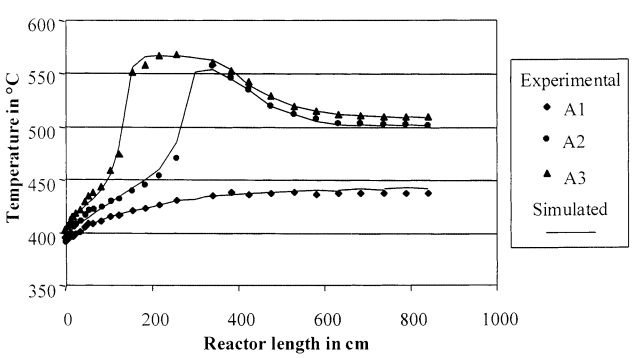

Fig. 2. Experimental and simulated temperature profiles for acetic acid hydrothermal oxidation with hydrogen peroxide at 25 MPa.

Table 2
Maximal temperature reached

Run	T_{max} (°C)
A1	438
A2	558
A3	568

of temperature profiles versus reactor length can be divided in three parts. The first one ($T_{injection} \leq T \leq 460$ °C) corresponded to the reaction initiation phase. The hydrogen peroxide decomposition and the first percent of acetic acid conversion (exothermic reaction) could explain the temperature increase. In a second part ($T \geq 460$ °C), the temperature increased rapidly. This temperature increase was explained by the combined effects of the water specific heat capacity decrease and the reaction kinetic rate acceleration. In fact, the water specific heat capacity decreased from 13.5 kJ kg^{-1} K^{-1} at 400 °C to 4.6 kJ kg^{-1} K^{-1} at 460 °C (25 MPa) [31]. Furthermore, the reaction kinetic rate increased by a factor 14 between 400 and 460 °C (activation energy of acetic acid oxidation reaction of 180 kJ mol^{-1} [6]). The maximal temperatures reached are reported in Table 2. When the maximal temperature was reached, acetic acid conversion into CO_2 and H_2O was quasi complete and the heat quantity released by the reaction was quasi null. So, in a third phase, the temperature decreased due to thermal loss according to the temperature gradient between reactive mixture and thermal shield.

Concerning the run A1, the temperature did not reach 460 °C during the reaction initiation phase because acetic acid concentration in the feed solution was too small.

Finally, these experimental temperature profiles locate the hot spot in the reactor and give the maximal temperature reached versus the initial acetic acid concentration. More the acetic acid concentration decreased, more the distance of the hot spot position from the reactor inlet increased.

A reactor model has been proposed to calculate the acetic acid global reaction heat from these experimental temperature profiles.

3.2. Reactor modeling

The quasi-adiabatic tubular reactor operated *at steady state*. The energetic balance of an open reactor in permanent working conditions is expressed as [32]:

$$\begin{pmatrix}\text{power}\\ \text{received}\\ \text{by the system}\end{pmatrix} = \begin{pmatrix}\text{heating}\\ \text{of mixture during}\\ \text{the reactor crossing}\end{pmatrix} + \begin{pmatrix}\text{heat adsorbed}\\ \text{by}\\ \text{chemical reactions}\end{pmatrix}$$

From this energetic balance, we have evaluated the global heat quantity released by the oxidation reaction in the experiment conditions studied. This global reaction heat takes into account the reaction enthalpy and the mixing enthalpies of the different compounds in the reactive mixture. With hydrogen peroxide as oxidant, the global reaction heat also includes the heat released by the hydrogen peroxide decomposition. In this paper, the global reaction heat will be noted ΔH_g.

The decomposition of this global reaction heat in its different terms (reaction enthalpy and mixing heat) was not investigated because the system was too complex even for the study of a model molecule like acetic acid. In fact, the reactive medium for the hydrothermal oxidation of acetic acid with hydrogen peroxide is already composed of numerous compounds (H_2O, CH_3COOH, CO_2, H_2O_2, byproducts of hydrogen peroxide decomposition [33], etc.). Furthermore, the scale up and the work of the process require only the knowledge of a global reaction heat.

A simulation work has shown that the quasi-adiabatic tubular reactor can be assimilated to *a plug flow reactor* in the studied conditions [25]. For a plug flow reactor, the energetic balance is performed on a slice of reactive mixture (Fig. 3) [32]:

$$\frac{\mathrm{d}q}{\mathrm{d}V_R} = U\frac{\mathrm{d}A}{\mathrm{d}V_R}(T_p - T) = F_0\Gamma_p\frac{\mathrm{d}T}{\mathrm{d}V_R} + F_A\frac{\mathrm{d}X}{\mathrm{d}V_R}\Delta H_g \quad (3)$$

where $\mathrm{d}q$ = power received by the reactor slice of volume $\mathrm{d}V_R$ from the exterior, U = global thermal transfer coefficient, $\mathrm{d}A$ = exchange surface of the reactor slice with the exterior, T_p = exterior temperature, T = temperature of the reactive mixture in the slice, F_0 = total molar flux, F_A = reagent molar flux, Γ_p = specific calorific capacity of reactive mixture, X = conversion rate of the reagent, and ΔH_g = global reaction heat.

First, we assumed that the thermodynamic properties of the reactive mixture could be assimilated to those of pure water. In fact, the concentration of organic load at the reactor inlet was lower than 5% in weight. That means:

$$\Gamma_p = Cp_{\text{water}}(T) \quad (4)$$

where $Cp_{\text{water}}(T)$ = specific calorific capacity of pure water versus temperature at constant pressure.

Second, the configuration of the reactor tube was such as only the half of the tube surface exchanged heat with exterior:

$$\frac{\mathrm{d}A}{\mathrm{d}V_R} = \frac{\Pi R\mathrm{d}L}{\Pi R^2\mathrm{d}L} = \frac{1}{R} \quad (5)$$

where R = tube radius, and $\mathrm{d}L$ = studied slice length. With these assumptions, the energetic balance on a reactive mixture slice in the quasi-adiabatic tubular reactor was:

$$\frac{U}{R}(T_p - T) = F_0 Cp_{\text{water}}(T)\frac{\mathrm{d}T}{\mathrm{d}V_R} + F_A\frac{\mathrm{d}X}{\mathrm{d}V_R}\Delta H_g \quad (6)$$

$(\mathrm{d}V_R = \Pi R^2\mathrm{d}L)$

Integrating Eq. (6) on the quasi-adiabatic tubular reactor length, we obtained:

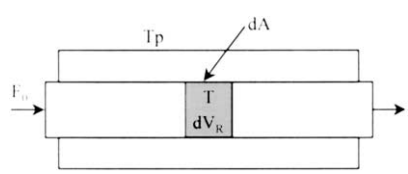

Fig. 3. Reactor model.

Table 3
Global reaction heat of acetic acid hydrothermal oxidation

Run	ΔH_g (kJ mol^{-1})
A1	−904.5
A2	−936.7
A3	−933.5

$$U\Pi R\int_0^L (T_p - T)\mathrm{d}L = F_0\int_0^L Cp_{water}(T)\frac{\mathrm{d}T}{\mathrm{d}L}\,\mathrm{d}L + F_A\Delta H_g\int_0^L \frac{\mathrm{d}X}{\mathrm{d}L}\,\mathrm{d}L \quad (7)$$

where L = the reactor length. Finally, the global heat quantity released by the reaction can be calculated from Eq. (7):

$$\Delta H_g = \frac{U\Pi R\int_0^L (T_p - T)\mathrm{d}L - F_0\int_0^L Cp_{water}(T)\frac{\mathrm{d}T}{\mathrm{d}L}\,\mathrm{d}L}{F_A X} \quad (8)$$

A software has been developed to calculate the global reaction heat from this equation and the experimental temperature profiles.

3.3. Determination of acetic acid global reaction heat

For all experiments, the Reynolds number was greater than 2200; so, the flow was turbulent in the reactor [32]. In these conditions, the quasi-adiabatic reactor can be assimilated to a plug flow reactor and Eq. (8), which is deduced from Eq. (3), can be used to calculate acetic acid global reaction heat.

The thermal transfer coefficient U was determined experimentally from runs performed with pure water and found equal to 26.5 W m^{-2} K^{-1}. It was assumed constant in our working conditions. The water specific calorific capacity function, $Cp_{water}(T)$, was determined from data base [31].

Starting from the experimental three temperature profiles and the reactor modeling, acetic acid global reaction heat was calculated. The results are reported in Table 3. Thus, the global reaction heat of acetic acid hydrothermal oxidation with hydrogen peroxide was evaluated at −925 kJ mol^{-1}. The heat quantity released by the hydrogen peroxide decomposition was included in this value and was equal to −15 kJ mol^{-1} with water as solvent.

The validation of this result was performed by a simulation of the reactor temperature profiles by a combination of the determined global reaction heat with kinetic data of the hydrothermal oxidation reaction of acetic acid [25].

The one-dimensional program solves the oxidation of model compounds in an adiabatic reactor at constant pressure or in a reactor cooling by convective heat transfer. The simulation results are shown in Fig. 2. The kinetic parameters were adjusted to fit the simulated temperature profiles to the experimental temperature profiles: preexponential factor equal to 85×10^9 s^{-1} and activation energy equal to 170 kJ mol^{-1}. These kinetic parameters are closed to those previously published: preexponential factor of 3.6×10^{11} s^{-1} and activation energy of 180 kJ mol^{-1} ($22.5 \le P \le 31$ MPa and $415 \le T \le 525$ °C) [34]. The simulation proves the validity of the obtained global reaction heat and the requirement of a such experimental reactor to scale up hydrothermal oxidation process.

4. Conclusions

Some parameters are necessary for scaling-up hydrothermal oxidation process (chemical pathway, reaction kinetic and thermal parameters, fluid thermodynamic properties, etc.). In this way, this paper was dedicated to the determination of hydrothermal oxidation global reaction heat from experimental investigations.

We have built a quasi-adiabatic tubular reactor to determine the heat quantity produced by the oxidation reaction. This reactor allows to obtain a temperature profile along its tube. A thermal modeling of the quasi-adiabatic tubular reactor was proposed to calculate global reaction heat from the experimental temperature profiles.

The experimental setup and the model were evaluated for acetic acid oxidation in supercritical water with hydrogen peroxide as oxidant. Besides

the calculation of global reaction heats, the experimental temperature profiles allow to locate the hot spot in the reactor and to determine the maximal temperature reached versus the initial acetic acid concentration.

The reaction heat of acetic acid hydrothermal oxidation with hydrogen peroxide was evaluated at -925 kJ mol^{-1}. A simulation of the temperature profiles along the reactor is in good agreement with the experimental temperature profiles. The main interest of the system, quasi-adiabatic tubular reactor and temperature profile analysis procedure, is the global reaction heat determination of complex wastes, which can not be evaluated by simulation.

To improve the simulation tool performances, we work on the determination of heat transfer coefficient in the reactor and the heat exchanger.

Acknowledgements

The authors thank the ECODEV program (CNRS) and the societies l'Electrolyse, Anjou Recherche and CNIM for their financial support.

References

[1] F. Cansell, P. Beslin, B. Berdeu, Hydrothermal oxidation of model molecules and industrial wastes, Env. Progr. 17 (4) (1998) 240.
[2] M. Modell, Processing method for the oxidation of organics in supercritical water, US Patent 4,338,199 (1982).
[3] E.F. Gloyna, L. Li, Progress in supercritical water oxidation: research, Chem. Oxid. 5 (1995) 1.
[4] H. Schmieder, J. Abeln, SCWO: facts and hopes, Wiss. Ber.-Forschungszent. Karlsruhe 6271 (1999) 83.
[5] C. Aymonier, P. Beslin, C. Jolivalt, F. Cansell, Hydrothermal oxidation of a nitrogen-containing compound: the fenuron, J. Supercrit. Fluids 17 (2000) 45.
[6] J.C. Meyer, P.A. Marrone, J.W. Tester, Acetic acid oxidation and hydrolysis in supercritical water, AIChE J. 41 (9) (1995) 2108.
[7] J.W. Tester, P.A. Webley, H.R. Holgate, Revised global kinetics measurements of methanol oxidation in supercritical water, Ind. Eng. Chem. Res. 32 (1993) 236.
[8] S. Gopalan, P.E. Savage, A reaction network model for phenol oxidation in supercritical water, AIChE J. 41 (8) (1995) 1864.
[9] N. Crain, S. Tebbal, L. Lixiong, E.F. Gloyna, Kinetics and reaction pathways of pyridine oxidation in supercritical water, Ind. Eng. Chem. Res. 32 (1993) 2259.
[10] M. Modell, J. Larson, S.F. Sobczynski, Supercritical water oxidation of pulp mill sludges, Tappi J. June (1992) 195.
[11] F. Cansell, S. Rey, P. Beslin, Thermodynamic aspects of supercritical fluids processing: applications to polymers and wastes treatment, Rev. Inst. Fr. Pétr. 53 (1) (1998) 71.
[12] E.U. Frank, S. Rosenzweig, M. Christoforakos, Calculation of the dielectric constant of water to 1000 °C and very high pressures, Ber. Bunsenges. Phys. Chem. 94 (1990) 199.
[13] W.L. Marshall, E.U. Frank, Ion product of water substance, 0–1000°C, 1–10000 bars — new international formulation and its background, J. Phys. Chem. Ref. Data 10 (2) (1981) 295.
[14] M.L. Japas, E.U. Frank, High pressure phase equilibria and PVT — Data of the water–oxygen system including water–air to 673 K and 250 MPa, Ber. Bunsenges. Phys. Chem. 89 (1985) 1268.
[15] J.F. Connolly, Solubility of hydrocarbons in water near the critical solution temperatures, J. Chem. Eng. Data 11 (1) (1966) 13.
[16] F.J. Armellini, J.W. Tester, Precipitation of sodium chloride and sodium sulfate in water from sub- to supercritical conditions: 150 to 550 °C, 100 to 300 bar, J. Supercrit. Fluids 7 (1994) 147.
[17] P. Kritzer, N. Boukis, E. Dinjus, Investigations of the corrosion of reactor materials during the process of Supercritical Water Oxidation (SCWO), in: The 6th Meeting on Supercritical Fluids: Chemistry and Materials, 1999, p. 433.
[18] C. Aymonier, B. Berdeu, F. Cansell, D. Sentagnes, Procédé de transformation de structures chimiques dans un fluide sous l'action des ultrasons et dispositif pour sa mise en œuvre, F Patent 98.08923 (1998).
[19] B. Berdeu, C. Aymonier, F. Cansell, D. Sentagnes, Procédé de transformation de structures chimiques dans un fluide sous pression et en température et dispositif pour sa mise en œuvre, F Patent 98.08923 (1998).
[20] C. Aymonier, M. Bottreau, B. Berdeu, F. Cansell, Ultrasound for hydrothermal treatments of aqueous wastes: solution for overcoming salt precipitation and corrosion, Ind. Eng. Chem. Res. 39 (2000) 4734.
[21] M.J. Cocero, J.L. Soria, O. Ganado, R. Gonzalez, F. Fdez-Polanco, Behaviour of a cooled wall reactor for supercritical water oxidation, in: R. von Rohr (Ed.), High Pressure Chemical Engineering, Elsevier Science, Oxford, 1996.
[22] V. Casal, H. Schmidt, SUWOX — a facility for the destruction of chlorinated hydrocarbons, J. Supercrit. Fluids 13 (1998) 269.
[23] Aerojet general corporation, Supercritical water oxidation reactor with wall conduits for boundary flow control, US Patent 5.387.398 (1995).

[24] C.H. Oh, R.J. Kochan, J.M. Beller, Numerical analysis and data comparison of a supercritical water oxidation reactor, Environ. Energy Eng. 43 (6) (1997) 1627.
[25] P. Dutournié, J. Mercadier, P. Cézac, Simulation of a tubular reactor for supercritical water oxidation, Rec. Prog. Génie Pr. 8 (70) (1999) 407.
[26] G. Petrich, J. Abeln, H. Schmieder, Model and simulation of supercritical water oxidation, High Pres. Chem. Eng. (1996) 157.
[27] P.E. Savage, M.A. Smith, Kinetics of acetic acid oxidation in supercritical water, Env. Sci. Tech. 29 (1) (1995) 216.
[28] L. Li, P. Chen, E.F. Gloyna, Kinetic model for wet oxidation of organic compounds in subcritical and supercritical water, Supercrit. Fluid Eng. Sci. 24 (1993) 306.
[29] P. Chen, L. Li, E.F. Gloyna, Simulation of a concentric-tube reactor for supercritical water oxidation, Inn. Supercrit. Fluids 24 (1995) 348.
[30] Prosim S.A., Prosim user's guide, 132 route d'Espagne, 31100 Toulouse, France.
[31] E. Schmidt, Properties of Water and Steam in SI-Units, Springer, New-York, 1982.
[32] J. Villermaux, Génie de la Réaction Chimique, TEC&DOC Lavoisier, London, 1995.
[33] E. Croiset, S.T. Rice, R.G. Hanush, Hydrogen peroxide decomposition in supercritical water, AIChE J. 43 (9) (1997) 2343.
[34] D.S. Lee, E.F. Gloyna, L. Li, Efficiency of H_2O_2 and O_2 in supercritical water oxidation of 2,4-dichlorophenol and acetic acid, J. Supercrit. Fluids 3 (4) (1990) 249.